



ELSEVIER

# Synthesis and characterization of zirconium pentafluorophenyl complexes: X-ray crystal structures of $[\text{ZrCl}_2(\text{C}_6\text{F}_5)_4]^{2-}$ and $[\text{ZrF}_2(\text{C}_6\text{F}_5)_5]^{3-}$

Melissa J. Nelsen, Gregory S. Girolami \*

School of Chemical Sciences, University of Illinois at Urbana-Champaign, 600 South Mathews Avenue, Urbana, IL 61801, USA

Received 8 March 1999

## Abstract

Treatment of  $\text{ZrCl}_4$  with  $\text{LiC}_6\text{F}_5$ , followed by addition of 1,4,7,10-tetraoxacyclododecane (12-crown-4) or *N,N,N',N'*-tetramethylethylenediamine (tmed), leads to the isolation of two pentafluorophenylzirconate complexes:  $[\text{Li}(12\text{-crown-4})_2]_2[\text{ZrCl}_2(\text{C}_6\text{F}_5)_4]$  (**1**) and  $[\text{Li}(\text{tmed})_2][\text{Li}(\text{tmed})_2][\text{ZrF}_2(\text{C}_6\text{F}_5)_5]$  (**2**). The presence of Zr–F groups in the latter compound shows that C–F bond activation has occurred. The anion in the former complex adopts an octahedral structure owing to the  $\pi$ -donor character of the chloride ligands, whereas the anion in the latter adopts a regular pentagonal bipyramidal structure. The lithium atoms in **1** are not interacting with the anion, whereas two of the lithium atoms in **2** are involved in  $\text{Li}\cdots\text{F}$  interactions with fluorine atoms in the anion. Selected bond distances and angles for **1**: Zr–C = 2.478(5)–2.510(5), Zr–Cl = 2.409(5), 2.435(5) Å, C–Zr–C(*cis*) = 77.9–106.9(2), C–Zr–C(*trans*) = 161.1, 169.1(2), Cl–Zr–Cl = 166.7(2)°. Selected bond distances and angles for **2**: Zr–C = 2.432–2.449(8), Zr–F = 1.986(4),  $\text{Li}\cdots\text{F}$  = 1.73(2)–2.50(2) Å, C–Zr–C(*cis*) = 69.6–73.3, F–Zr–F = 178.8(2)°. Crystal data for **1**: monoclinic, space group  $P2_1/n$ ,  $a$  = 15.2288(14),  $b$  = 17.328(2),  $c$  = 24.013(2) Å,  $\beta$  = 91.936(3)°,  $V$  = 6333(1) Å<sup>3</sup>,  $Z$  = 4,  $wR_2$  = 0.2985 for 7801 reflections and 722 parameters. Crystal data for **2**: monoclinic, space group  $P2_1/n$ ,  $a$  = 11.6143(5),  $b$  = 29.6561(9),  $c$  = 20.4427(8) Å,  $\beta$  = 103.266(1)°,  $V$  = 6853.3(4) Å<sup>3</sup>,  $Z$  = 4,  $wR_2$  = 0.1822 for 8762 reflections and 759 parameters. © 1999 Elsevier Science S.A. All rights reserved.

**Keywords:** Zirconium; Group 4; Carbon–fluorine bond activation; Seven-coordination; Pentafluorophenyl

## 1. Introduction

In 1972, Wilkinson announced the synthesis of the remarkable compound hexamethyltungsten ( $\text{WMe}_6$ ) [1]. Ever since, this compound has served as the archetypal example of a binary transition metal alkyl. For many years, it was thought to possess an octahedral structure, and this supposition was accepted without question [2–4].

In 1989, we described the synthesis and characterization of the hexamethylzirconate salt  $[\text{Li}(\text{tmed})_2][\text{ZrMe}_6]$ , and showed that it adopts a trigonal prismatic structure [5]. The anion in this salt is involved in weak interactions with the lithium cations, and a natural question to ask is whether the cation–anion interactions stabilize

the trigonal prismatic geometry. It has been suggested that capping the trigonal face or bridging a square edge would enhance the preference for a trigonal prism, but the lithium cations in  $[\text{Li}(\text{tmed})_2][\text{ZrMe}_6]$  are located in neither of these sites; instead they bridge one of the trigonal edges. Furthermore, analogous  $d^3$  complexes such as  $[\text{Li}(\text{Et}_2\text{O})_4][\text{VPh}_6]$  [6],  $[\text{Li}(\text{Et}_2\text{O})_3][\text{CrPh}_6]$  [6], and  $[\text{Li}(\text{tmed})_2][\text{MnMe}_6]$  [7] manage to adopt the expected octahedral structure despite having similar  $\text{Li}\cdots\text{C}$  interactions. These observations suggest that the  $\text{Li}\cdots\text{C}$  interactions are not controlling the structure of  $[\text{ZrMe}_6]^{2-}$ . Instead, the non-octahedral geometry seen for the hexamethylzirconate(IV) dianion reflects an intrinsic electronic driving force to lower the symmetry [5,8]. We pointed out that  $\text{WMe}_6$  should be trigonal prismatic for similar reasons, and this expectation was subsequently verified by gas phase electron diffraction [9] and X-ray crystallographic studies [10].

\* Corresponding author.

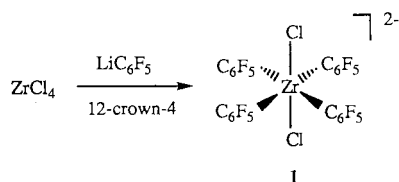
To remove all doubts about the reasons for the trigonal prismatic structure of  $[\text{ZrMe}_6^{2-}]$ , it would be of interest to prepare  $[\text{ZrR}_6^{2-}]$  salts in which  $\text{Li}\cdots\text{C}$  contacts with the cations were completely absent in the solid state. Metal-coordinated alkyl and aryl ligands bear partial negative charges on the  $\alpha$ -carbon atoms, so it is not surprising that lithium cations would be found within bonding distance of these atoms. In metal complexes of fluoroalkyl or fluoroaryl ligands, however, the electron density on the  $\alpha$ -carbon should be reduced and the electrostatic attraction for the lithium cations should be reduced as well. A salt of a  $[\text{ZrR}_6^{2-}]$  anion that lacks  $\text{Li}\cdots\text{C}$  interactions might then be isolable; although  $\text{Li}\cdots\text{F}$  interactions may still be present. Therefore, in an attempt to prepare a  $d^0$  zirconium homoleptic species that lacks  $\text{Li}\cdots\text{C}$  interactions, we investigated the synthesis of zirconium complexes of the pentafluorophenyl ligand. While we have not yet been successful in synthesizing the  $[\text{Zr}(\text{C}_6\text{F}_5)_6^{2-}]$  anion, our attempts to do so have afforded two new pentafluorophenylzirconate salts with interesting structures.

## 2. Results

### 2.1. Synthesis and crystal structure of $[\text{Li}(\text{12-crown-4})_2][\text{ZrCl}_2(\text{C}_6\text{F}_5)_4]$

In the present study, pentafluorophenyllithium was used to deliver  $\text{C}_6\text{F}_5$  groups to  $\text{ZrCl}_4$ . The  $\text{LiC}_6\text{F}_5$  reagent can be synthesized by the low temperature reaction of bromopentafluorobenzene with either *n*-butyllithium or lithium amalgam [11]. In the present investigation, however, we employed a halide-free route to prepare  $\text{LiC}_6\text{F}_5$ : treatment of pentafluorobenzene with *n*-butyllithium at low temperatures [12].

Treatment of  $\text{ZrCl}_4$  with  $\text{LiC}_6\text{F}_5$  in diethylether at  $-20^\circ\text{C}$ , followed by the addition of 12-crown-4, yields a colorless solution from which colorless crystals of the new compound  $[\text{Li}(\text{12-crown-4})_2][\text{ZrCl}_2(\text{C}_6\text{F}_5)_4]$  (**1**) may be obtained.



Although we had intended to replace all of the chloride groups attached to the zirconium center, the stoichiometry of the isolated product suggests that some of the pentafluorophenyllithium reagent had decomposed during the reaction. As a solid, **1** is stable at room temperature (r.t.) for several hours and at  $-20^\circ\text{C}$  for several weeks. In solution, however, decomposition occurs within minutes at r.t.

Compound **1** is insoluble in hydrocarbon solvents, and only sparingly soluble in cold diethylether and cold THF. For these reasons, satisfactory NMR results could not be obtained: at high temperatures the compound decomposes, and at low temperatures it is insoluble.  $^1\text{H}$ - and  $^{19}\text{F}$ -NMR spectra of solutions prepared by the low-temperature dissolution of **1** feature peaks due to free 12-crown-4 and the hydrolysis (or decomposition) product pentafluorobenzene. No peaks were present that could be unambiguously attributed to intact molecules of **1**.

Crystals of **1**, grown from diethylether, crystallize in the monoclinic space group  $P2_1/n$  with four molecules in the unit cell; one molecule is present in the asymmetric unit. Crystal data are presented in Table 1 and selected bond distances and angles are collected in Table 2. ORTEP diagrams of the molecular structure are shown in Figs. 1 and 2.

Crystals of **1** consist of discrete cations and anions with the following features. The zirconium center adopts a distorted octahedral geometry in which the two chlorine atoms are mutually *trans*. The orientations of the  $\text{C}_6\text{F}_5$  rings with respect to the  $\text{ZrCl}_2$  plane differ: two are essentially perpendicular to this plane, and two

Table 1

Crystal data<sup>a</sup> for  $[\text{Li}(\text{12-crown-4})_2][\text{ZrCl}_2(\text{C}_6\text{F}_5)_4]$  (**1**) and  $[\text{Li}(\text{tmed})_2][\text{Li}(\text{tmed})_2][\text{ZrF}_2(\text{C}_6\text{F}_5)_5]$  (**2**)

Compound	1	2
Formula	$\text{C}_{56}\text{H}_{64}\text{Cl}_2\text{F}_{20}\text{Li}_2\text{O}$	$\text{C}_{56}\text{H}_{69}\text{F}_{27}\text{Li}_3\text{N}_8\text{O}$
$M_r$	1549.07	1487.24
Crystal system	Monoclinic	Monoclinic
Space group	$P2_1/n$	$P2_1/n$
<i>a</i> (Å)	15.2288(14)	11.6143(5)
<i>b</i> (Å)	17.328(2)	29.6561(9)
<i>c</i> (Å)	24.013(2)	20.4427(8)
$\beta$ (°)	91.936(3)	103.266(1)
<i>V</i> (Å <sup>3</sup> )	6333(1)	6853.3(4)
<i>Z</i>	4	4
$D_{\text{calc}}$ (g cm <sup>-3</sup> )	1.625	1.441
<i>F</i> (000)	3152	3028
Crystal size (mm)	0.30 × 0.12 × 0.04	0.30 × 0.20 × 0.10
$\mu$ (Mo-K $\alpha$ ) (mm <sup>-1</sup> )	0.383	0.276
Max./min. transmission	0.941, 0.874	0.940, 0.812
Maximum $2\theta$ (°)	44.2	45
No. unique reflections	7805	8967
No. used in refinement, $N_o$	7801	8762
No. observed data [ $F_o^2 > 2\sigma(F_o^2)$ ]	2252	3692
No. parameters refined, $N_p$	722	759
$R_1$ (observed data)	0.1022	0.0700
$wR_2$ (all data)	0.2985	0.1822
Goodness of fit on $F^2$	1.011	0.990
Maximum $\Delta/\sigma$	0.004	0.002
Maximum $\Delta\rho$ (e Å <sup>-3</sup> )	0.60	0.57

<sup>a</sup>  $R_1 = \sum ||F_o| - |F_c|| / \sum |F_o|$ ,  $wR_2 = [\sum w(F_o^2 - F_c^2)^2 / \sum w(F_o^2)]^{1/2}$ , goodness of fit =  $[\sum w(F_o^2 - F_c^2)^2 / (N_o - N_p)]^{1/2}$ . Weighting scheme  $w = [\sigma^2(F_o^2) + (aP)^2 + bP]^{-1}$ , where  $P = [\max(F_o^2, 0) + 2F_c^2]/3$ .

Table 2  
Selected bond distances (Å) and angles (°) for compound **1** with estimated S.D. values in parentheses

Zr–Cl(1)	2.409(5)	Li(1)–O(62)	2.10(4)
Zr–Cl(2)	2.435(5)	Li(1)–O(63)	2.13(4)
		Li(1)–O(64)	2.26(4)
Zr–C(11)	2.479(5)	Li(2)–O(71)	2.40(4)
Zr–C(21)	2.478(5)	Li(2)–O(72)	2.29(4)
Zr–C(31)	2.510(5)	Li(2)–O(73)	2.41(4)
Zr–C(41)	2.495(5)	Li(2)–O(74)	2.30(4)
Li(1)–O(52)	2.18(4)	Li(2)–O(81)	2.40(5)
Li(1)–O(53)	2.20(4)	Li(2)–O(82)	2.42(5)
Li(1)–O(61)	2.24(4)	Li(2)–O(83)	2.23(5)
		Li(2)–O(84)	2.36(5)
Cl(1)–Zr–Cl(2)	166.7(2)	Cl(2)–Zr–C(31)	93.9(2)
		Cl(2)–Zr–C(41)	82.8(2)
Cl(1)–Zr–C(11)	96.1(2)	C(11)–Zr–C(21)	161.1(2)
Cl(1)–Zr–C(21)	83.1(2)	C(11)–Zr–C(31)	77.9(2)
Cl(1)–Zr–C(31)	97.8(2)	C(11)–Zr–C(41)	91.8(2)
Cl(1)–Zr–C(41)	86.8(2)	C(21)–Zr–C(31)	83.5(2)
Cl(2)–Zr–C(11)	92.4(2)	C(21)–Zr–C(41)	106.9(2)
Cl(2)–Zr–C(21)	92.1(2)	C(31)–Zr–C(41)	169.1(2)

lie nearly in this plane. Interestingly, the two that lie essentially in the plane are mutually *cis*, and the angle between them is expanded to 106.9(2)°. The two aryl ligands that are perpendicular to the ZrC<sub>4</sub> plane are also mutually *cis*, and the 77.9(2)° angle between these two ligands is the smallest interligand angle in the anion. The chlorine atoms are canted slightly away from the latter pair of ligands to accommodate the steric demands of the *ortho*-fluorine atoms on the more nearly vertical rings. As a result, the Cl–Zr–Cl angle of 166.7(2)° also deviates from the ideal value for an octahedron.

The average zirconium–carbon bond length is

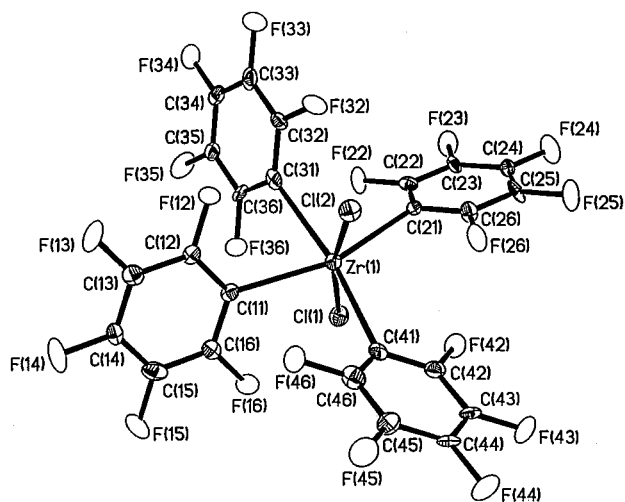


Fig. 1. ORTEP drawing of  $[\text{ZrCl}_2(\text{C}_6\text{F}_5)_4]^{2-}$  anion in **1**. The 20% probability density surfaces are shown.

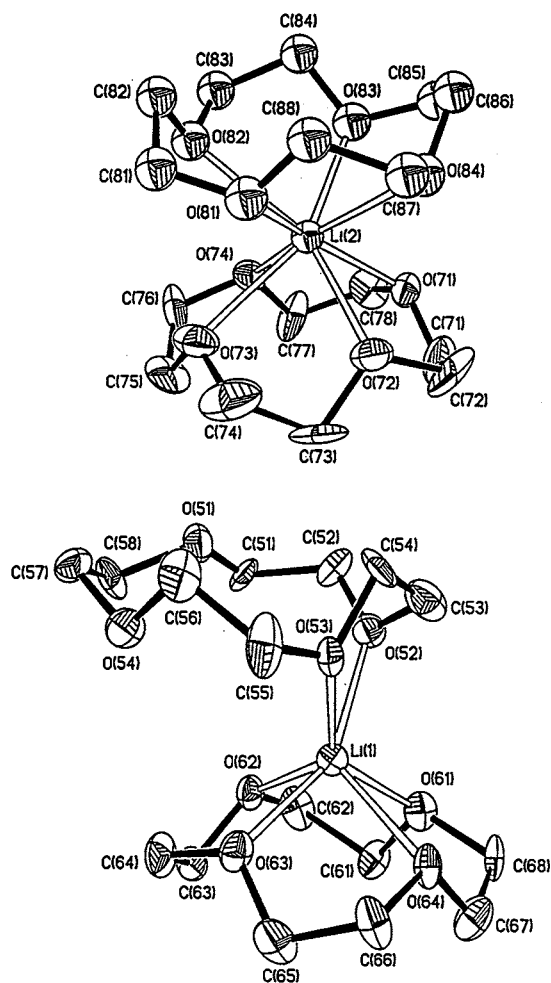


Fig. 2. ORTEP drawing of the two charge-separated  $[\text{Li}(12\text{-crown-4})_2]^{2+}$  cations in **1**. The 20% probability density surfaces are shown.

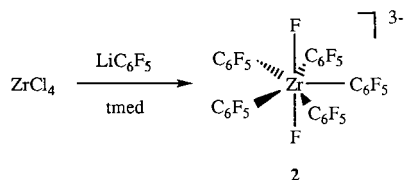
2.490(5) Å. The zirconium–chlorine bond lengths are 2.409(5) and 2.435(5) Å. A similar Zr–Cl bond distance of 2.44 Å is found for the metallocene  $\text{Cp}_2\text{ZrCl}_2$  [13].

Each lithium atom is coordinated to two 12-crown-4 molecules, as is often seen [14]. The two cations, however, exhibit very different geometries. One lithium atom is eight-coordinate and is bound to all of the oxygen atoms of the two crown ethers. In this cation, one of the two crown ethers is disordered over two conformers. The average Li–O bond distance in this cation is 2.35(4) Å and individual values range from 2.23(5) to 2.42(5) Å. Similar Li–O bond lengths have been reported for other bis(12-crown-4)lithium cations: for example, in  $[\text{Li}(12\text{-crown-4})_2][\text{Me}_3\text{SiC}_3\text{H}_5]$  the Li–O bond lengths average 2.366(9) Å and range from 2.271(9) to 2.531(9) Å [15]. In contrast, the other lithium cation in the structure of **1** is six-coordinate; it is bound to four oxygen atoms of one crown ether but to only two oxygen atoms of the second. The Li–O bond distances, which average 2.18(4) Å and range from 2.10(4) to 2.24(4) Å, are slightly shorter than

those seen for its eight-coordinate counterpart. Comparable Li–O bond distances have been reported for a lithium cation in a similar six-coordinate environment: the Li–O bond lengths in [Li(12-crown-4)][N(SO<sub>2</sub>CH<sub>3</sub>)<sub>2</sub>] average 2.118(4) Å and range from 2.036(4) to 2.215(4) Å [16].

## 2.2. Synthesis and crystal structure of [Li(tmed)<sub>2</sub>][Li(tmed)]<sub>2</sub>[ZrF<sub>2</sub>(C<sub>6</sub>F<sub>5</sub>)<sub>5</sub>]

Treatment of ZrCl<sub>4</sub> with excess LiC<sub>6</sub>F<sub>5</sub> in diethylether at –20°C, followed by the addition of tmed yields a blue solution from which colorless crystals of [Li(tmed)<sub>2</sub>][Li(tmed)]<sub>2</sub>[ZrF<sub>2</sub>(C<sub>6</sub>F<sub>5</sub>)<sub>5</sub>] (**2**) may be isolated.



The blue color indicates the formation of decomposition products from the C<sub>6</sub>F<sub>5</sub> group. In contrast to the results described above, all of the chloride atoms of the ZrCl<sub>4</sub> starting material have been replaced. Even so, the product is not a hexa(aryl) compound, and instead the zirconium center bears two fluoride ligands.

As a solid, **2** is stable for several hours at r.t. and indefinitely at –20°C; it is insoluble in hydrocarbons, sparingly soluble in diethylether, and soluble in THF.

Crystals of **2**, grown from diethylether, conform to the monoclinic space group *P*2<sub>1</sub>/*n* with four molecules in the unit cell and one molecule in the asymmetric unit. Crystal data are presented in Table 1 and selected bond distances and angles are collected in Table 3. ORTEP diagrams of the molecular structures are shown in Figs. 3 and 4.

The zirconium center in the [ZrF<sub>2</sub>(C<sub>6</sub>F<sub>5</sub>)<sub>5</sub>]<sup>3–</sup> anion adopts a nearly ideal pentagonal bipyramidal structure in which the two fluorine atoms occupy the axial positions and the pentafluorophenyl ligands are arranged in a pinwheel fashion in the equatorial positions. The C–Zr–C angles average 72.08°, and the F–Zr–F angle is 178.8°. In comparison, the interligand bond angles for an ideal pentagonal bipyramid are 72° between the equatorial ligands, and 180° between the two axial ligands. Crystallographically characterized examples of pentagonal bipyramidal geometries are remarkably rare for molecular zirconium complexes, and no other examples of seven-coordinate organozirconium compounds with exclusively σ-bonded ligands have been reported. The seven-coordinate complex Zr(acac)<sub>3</sub>Cl adopts a pentagonal bipyramidal geometry, but the pentagonal girdle is significantly buckled [17]. Several crystallographic studies of salts of the [ZrF<sub>7</sub><sup>3–</sup>] ion have been carried out. The [ZrF<sub>7</sub><sup>3–</sup>] anion

Table 3

Selected bond distances (Å) and angles (°) for compound **2** with estimated S.D. values in parentheses

Zr–F(1)	1.987(4)	Li(1)–N(1)	2.14(2)
Zr–F(2)	1.985(4)	Li(1)–N(2)	2.13(2)
Zr–C(11)	2.447(9)	Li(2)–F(2)	1.73(2)
Zr–C(21)	2.449(8)	Li(2)–F(46)	2.50(2)
Zr–C(31)	2.437(8)	Li(2)–F(56)	2.34(2)
Zr–C(41)	2.446(9)		
Zr–C(51)	2.432(9)	Li(2)–N(3A)	2.10(2)
		Li(2)–N(4A)	2.31(2)
Li(1)–F(1)	1.77(2)		
Li(1)–F(32)	2.140(14)	Li(3)–N(5)	2.09(2)
Li(1)–F(42)	2.43(2)	Li(3)–N(6)	2.10(2)
		Li(3)–N(7)	2.16(2)
		Li(3)–N(8)	2.19(2)
F(1)–Zr–F(2)	178.8(2)	C(11)–Zr–C(21)	73.3(3)
F(1)–Zr–C(11)	90.1(2)	C(11)–Zr–C(31)	145.2(3)
F(1)–Zr–C(21)	91.6(2)	C(11)–Zr–C(41)	142.7(3)
F(1)–Zr–C(31)	86.7(2)	C(11)–Zr–C(51)	73.2(3)
F(1)–Zr–C(41)	91.7(3)	C(21)–Zr–C(31)	72.2(3)
F(1)–Zr–C(51)	88.8(3)	C(21)–Zr–C(41)	143.8(3)
F(2)–Zr–C(11)	89.9(3)	C(21)–Zr–C(51)	146.5(3)
F(2)–Zr–C(21)	89.6(2)	C(31)–Zr–C(41)	72.1(3)
F(2)–Zr–C(31)	93.9(2)	C(31)–Zr–C(51)	141.2(3)
F(2)–Zr–C(41)	87.5(3)	C(41)–Zr–C(51)	69.6(3)
F(2)–Zr–C(51)	90.0(3)		

in [NH<sub>4</sub>]<sub>3</sub>[ZrF<sub>7</sub>] is thought to have a pentagonal bipyramidal structure, but the anions are dynamically disordered [18]. Crystallographic examination of [enH<sub>2</sub>]<sub>3</sub>[ZrF<sub>7</sub>]<sub>2</sub>·2H<sub>2</sub>O reveals the presence of two inde-

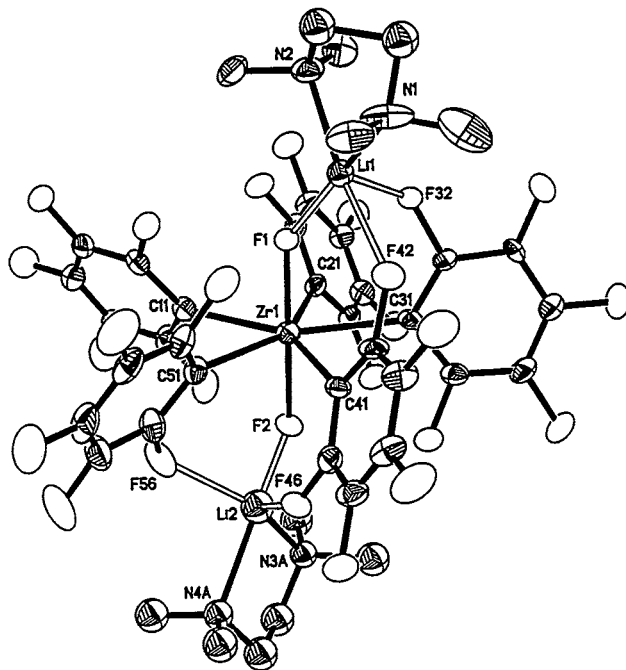


Fig. 3. ORTEP drawing of the [ZrF<sub>2</sub>(C<sub>6</sub>F<sub>5</sub>)<sub>5</sub>]<sup>3–</sup> anion in **2** with associated [Li(tmed)<sup>+</sup>] cations. The 20% probability density surfaces are shown. The charge-separated [Li(tmed)<sub>2</sub><sup>+</sup>] cation is not illustrated but has the expected distorted tetrahedral geometry.

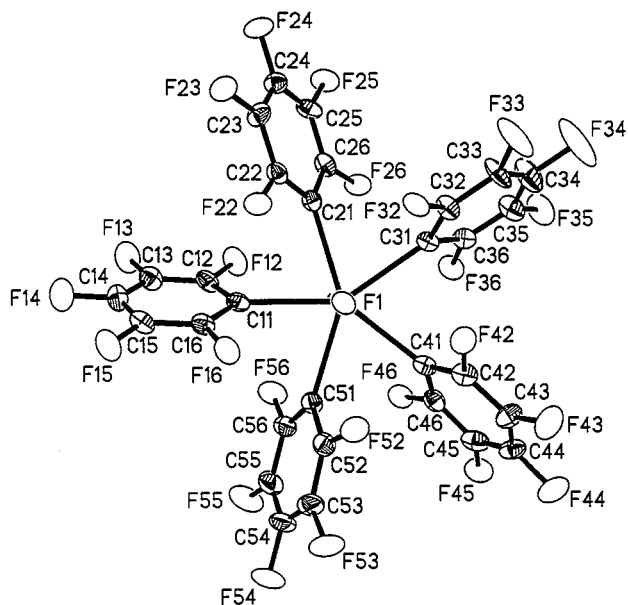


Fig. 4. ORTEP drawing of the  $[\text{ZrF}_2(\text{C}_6\text{F}_5)_3]^{2-}$  anion in **2**, viewed down the pseudo-five-fold axis. The 20% probability density surfaces are shown.

pendent heptafluorozirconate anions, both of which adopt capped trigonal prismatic geometries [19].

The Zr–F bond lengths in the  $[\text{ZrF}_2(\text{C}_6\text{F}_5)_3]^{2-}$  anion are 1.985(4) and 1.987(4) Å; these distances are essentially equal to those of 1.98 and 2.002 Å reported for  $\text{Cp}_2\text{ZrF}_2$  [20] and  $(\text{C}_5\text{Me}_4\text{Et})_2\text{ZrFCl}$  [21]. Crystallographic examinations of the  $[\text{ZrF}_7]^{3-}$  ion give average Zr–F bond lengths which are somewhat longer: 2.061 Å for  $[\text{NH}_4]_3[\text{ZrF}_7]$  [18], 2.035 Å for  $[\text{C}_2\text{N}_2\text{H}_{10}]_3[\text{ZrF}_7]$  [19], and 2.090 Å for  $\text{Rb}_5\text{Zr}_4\text{F}_{21}$  [22]. Much longer Zr–F bond lengths of 2.212 Å are present in  $[\eta\text{-C}_5\text{H}_3(\text{SiMe}_2)_2]_2\text{ZrF}_2$  [23].

The axial groups in the anion have been identified as fluoride groups, but we must consider the possibility that they are hydroxide groups instead. Fluoride and hydroxide are essentially indistinguishable crystallographically unless the hydrogen atom of the OH group can be located, which is not the case here. Several pseudo eight-coordinate zirconium complexes containing hydroxide groups are known [24–26], and the Zr–O distances of 1.950(2) to 2.00(2) Å are similar to the Zr–F distances in **2**. Although adventitious water could provide a source of hydroxide, the simpler hypothesis is that the  $\text{C}_6\text{F}_5$  groups serve as a source of fluoride, as they often do in other systems (see below).

The average zirconium–carbon bond length is 2.442(9) Å. This value is slightly shorter than that seen in  $[\text{ZrCl}_2(\text{C}_6\text{F}_5)_4]^{2-}$ , probably because there are no ligands directly *trans* to the  $\text{C}_6\text{F}_5$  groups in the  $[\text{ZrF}_2(\text{C}_6\text{F}_5)_3]^{2-}$  anion, so that the bonds are not lengthened by a *trans*-influence.

Of the three lithium atoms per formula unit, two are involved in ion-pair interactions with the  $[\text{ZrF}_2(\text{C}_6\text{F}_5)_3]^{2-}$  anion, while the third is not. Each of the two ion-paired lithium atoms interacts with a zirconium-bound fluorine atom, two ring fluorines, and a tmed molecule. The geometries about these lithium atoms are best described as distorted square pyramids with a ring fluorine atom in the axial site. The strongest interaction is between lithium and the zirconium-bound fluorine atom as evidenced by the short Li–F contact distances of 1.73(2) and 1.77(2) Å. The average Li–F distance to the ring fluorines of 2.35(5) Å is considerably longer. This difference in bond lengths is probably attributable to the greater attraction of the lithium cation toward the larger partial negative charge on the fluoride atoms that are attached directly to the zirconium center.

The third lithium cation, which is charge-separated from the zirconium anion, is bound to two tmed molecules in a tetrahedral environment. The Li–N bond distances of 2.13(2) Å are very similar in the ion-paired and charge-separated lithium centers. Similar Li–N distances are seen in other lithium–tmed complexes [27–29].

Finally, we note that attempts to isolate salts of the hexakis(pentafluorophenyl)zirconate dianion in the absence of 12-crown-4 or tmed result in the formation of a yellow brown substance that detonates spontaneously under vacuum at low temperature.

### 3. Discussion

#### 3.1. The metal–pentafluorophenyl bond

Many authors have noted that there are significant differences between phenyl complexes and their pentafluorophenyl analogs. Organotransition metal compounds that contain perfluorinated organic ligands are often more thermally robust than their hydrocarbon analogs. The enhanced stability of these compounds has been attributed to  $\pi$  back bonding from the transition metal center to the  $\alpha$ -carbon of the perfluorocarbon ligand [30].

Evidence in favor of  $\pi$  back bonding to fluoroalkyl ligands comes from comparisons of C–F force constants calculated from IR spectra. For molecules of the type  $\text{CF}_3\text{X}$ , the force constants reveal that the C–F bond weakens when the trifluoromethyl group is coordinated to a metal center (e.g.  $\text{X} = \text{Mn}(\text{CO})_5$ ) [31]. The weakening of the C–F bond is best attributed to electron donation from the metal atom to the C–F antibonding orbitals. Additional evidence of multiple bond character between transition metal atoms and the carbon atoms of perfluorocarbon groups comes from the observation that the metal–carbon bond lengths are

often shorter for perfluorocarbon derivatives than for their hydrocarbon analogs [32,33].

Not all the evidence, however, supports the hypothesis that  $\pi$  back bonding effects are characteristic of perfluoroalkyl and -aryl ligands. For instance, the Au–C bonds in  $[\text{N}(\text{PPh}_3)_2][\text{Au}(\text{C}_6\text{F}_5)_4]$  show no evidence of multiple bond character [34]. Similar findings have been reported for  $\text{Ir}(\text{CO})(\text{C}_6\text{F}_5)(\text{PPh}_3)_2$  [35].

In contrast to the relative abundance of late transition metal perfluoroaryl compounds, few early transition metal complexes containing such ligands are known. Both  $\text{Cp}_2\text{Ti}(\text{C}_6\text{F}_5)_2$  and  $\text{Cp}_2\text{Ti}(\text{C}_6\text{F}_5)\text{Cl}$  are stable in air and do not decompose below 200°C; these compounds are considerably more robust than their phenyl analogs, which are air-sensitive and decompose slowly at r.t. even under vacuum [36]. Tetrakis(pentafluorophenyl)titanium(IV) has also been reported, and although the characterization of this compound leaves much to be desired, the authors claimed that the complex is more thermally stable than its hydrocarbon analog  $\text{TiPh}_4$  [37]. More recently, a  $\text{Ti}-\text{C}_6\text{F}_5$  complex has been prepared by activation of a B–C bond in  $\text{B}(\text{C}_6\text{F}_5)_3$  [38].

For the new compounds **1** and **2**, the average Zr– $\text{C}_6\text{F}_5$  bond distances are 2.490(5) and 2.442(9) Å, respectively. Interestingly, these bonds are significantly longer than the Zr–C bonds in related arylzirconate(IV) complexes. For example, the Zr–C bond lengths to the *p*-tolyl ligand in  $[(\eta^8-\text{C}_8\text{H}_8)\text{Zr}(\text{p}-\text{C}_6\text{H}_4\text{Me})\text{Cl}_2]^-$  and to the phenyl ligands in trigonal prismatic  $[\text{ZrPh}_6]^{2-}$  are 2.329(6) and 2.363(7) Å, respectively [39]. This trend is the opposite of that observed for aryl versus perfluoroaryl complexes of the later transition metals.

The lengthening of the Zr–C bonds in **1** and **2** relative to those in arylzirconate(IV) complexes cannot be a consequence of metal-to-ligand  $\pi$  back bonding, because the metal centers are  $d^0$ . Instead, the lengthening may be the result of increased interligand repulsions due to the fluorine substituents: the anions in **1** and **2** are both reasonably crowded, the pentakis(pentafluorophenyl) compound **2** especially so due to the higher coordination number of this complex. Another factor that may contribute to the lengthening of the Zr–C bonds in **1** (but not in **2**) is a *trans* influence: only in **1** are the  $\text{C}_6\text{F}_5$  groups directly *trans* to another  $\sigma$ -bonding ligand.

### 3.2. Six-coordinate geometries

The trigonal prismatic structure of the hexamethylzirconate salt  $[\text{Li}(\text{tmed})_2][\text{ZrMe}_6]$  violates the prediction of points-on-a-sphere models. It can be understood, however, in terms of a second-order Jahn–Teller effect in which lowering the symmetry from  $O_h$  to  $D_{3h}$  improves the metal–ligand sigma bonding [5–8].

The symmetry-lowering is only stabilizing when the ligands lack  $\pi$ -donor character; thus alkyl groups, hydrides, and certain neutral Lewis bases will favor trigonal prismatic geometries, while halide, alkoxide, and amide ligands will favor octahedral geometries when bound to  $d^0$  metal centers.

The present study reveals that the  $[\text{ZrCl}_2(\text{C}_6\text{F}_5)_4]^-$  anion is essentially octahedral. Evidently, the chloride-to-metal  $\pi$ -donor interactions are sufficient to stabilize the octahedral geometry of the present molecule probably relative to the trigonal prismatic geometry. Thus, even if only two of the six ligands about a  $d^0$  metal center are  $\pi$ -donors, an octahedral geometry is likely to be the lowest energy. This conclusion has relevance to heterogeneous Ziegler–Natta catalysts, in which the active sites are thought to be electron-deficient metal centers ligated by both chloride and alkyl groups. Specifically, the reactive sites in these heterogeneous catalysts probably do adopt pseudo-octahedral geometries, as is invariably assumed, provided that at least some chloride ligands are in the coordination sphere.

### 3.3. Seven-coordinate geometries

The pentagonal bipyramidal geometry is only one of the geometries possible for seven-coordinate compounds. Others include the capped octahedron and the capped trigonal prism. Early MO calculations found that all three geometries had roughly equal energies [40]. More recent MO calculations suggest that the latter two geometries are the most stable for transition metal compounds, while the pentagonal bipyramidal geometry is most stable for main group compounds [41]. Ligand repulsion models also find all three geometries to be approximately equal in energy, but the pentagonal bipyramid is slightly favored for compounds of the type  $[\text{M}(\text{unidentate A})_5(\text{unidentate B})_2]$  as in compound **2** [42].

In the  $[\text{ZrF}_2(\text{C}_6\text{F}_5)_3]^-$  ion, the Zr–F bond lengths (1.986 Å) are considerably shorter than the Zr–C bond lengths (2.442 Å), and thus the most sterically demanding ligands in the innermost coordination sphere are the fluoride ligands. These atoms will therefore occupy the least sterically hindered positions, which in a pentagonal bipyramid are the axial sites.

### 3.4. Carbon–fluorine bond activation

The appearance of zirconium-bound fluoride ligands in **2** shows that carbon–fluorine bond activation must have taken place. Carbon–fluorine bonds are stronger than carbon–hydrogen bonds and are correspondingly more difficult to activate [30,43,44]. Nevertheless, many transition metal complexes promote C–F bond activation [30]. Although some lanthanide complexes have shown surprising reactivity [45,46], most of the C–F

bond activation processes observed to date involve late transition metal compounds. For example, the complex  $\text{Rh}(\text{SiMe}_2\text{Ph})(\text{PMe}_3)_3$  promotes the reaction of hydrosilanes with hexafluorobenzene to give fluorosilanes and pentafluorobenzene [47–50].

The reaction of hexafluorobenzene with late transition metal complexes to yield products with pentafluorophenyl groups is relatively common [30]. It is generally believed that the carbon–fluorine bonds are weakened when the fluorocarbon binds to a late transition metal center; this effect is ascribed to donation of electron density into the C–F antibonding orbitals.

The bonding situation is different for  $d^0$  metal centers because they cannot  $\pi$  back bond in the same fashion as late transition metals. Instead, for early transition metals, the activation of carbon–fluorine bonds probably proceeds in a fashion similar to the activation of carbon–hydrogen bonds. For example, thermolysis of  $\text{Cp}_2\text{Ti}(\text{C}_6\text{F}_5)_2$  produces  $\text{Cp}_2\text{TiF}(\text{C}_6\text{F}_5)$  [36]. In comparison, thermolysis of  $\text{Cp}_2^*\text{ZrPh}_2$  yields the ‘tuck-in’ complex  $\text{Cp}^*\text{Zr}(\text{C}_5\text{Me}_4\text{CH}_2)\text{Ph}$  [51]. No other examples of the activation of the C–F bonds of pentafluorophenyl ligands by early transition metals have been reported.

The chemistry that leads to cleavage of the C–F bond and production of  $[\text{Li}(\text{tmed})_2][\text{Li}(\text{tmed})_2\text{-ZrF}_2(\text{C}_6\text{F}_5)_5]$  may be very similar to that involved in the conversion of  $\text{Cp}_2\text{Ti}(\text{C}_6\text{F}_5)_2$  to  $\text{Cp}_2\text{TiF}(\text{C}_6\text{F}_5)$ . We noted that addition of tmed to the pale yellow  $\text{ZrCl}_4/\text{LiC}_6\text{F}_5$  solution caused the solution to turn blue. One explanation of this color change is that the hexakis(pentafluorophenyl)zirconate dianion is generated in the initial reaction, but that addition of the strongly-coordinating tmed ligands disrupts the stabilizing interaction between the zirconate anion and the lithium cations, thus instigating the C–F bond cleavage process that leads to the formation of **1**. The blue color marks the formation of unidentified perfluoro-organic side products generated by the C–F bond cleavage step.

We cannot rule out the possibility, however, that C–F bond activation occurs before alkylation of the metal center, i.e. while the  $\text{C}_6\text{F}_5$  group is present as an organolithium reagent. Pentafluorophenyllithium cannot be isolated, and it readily decomposes even at low temperature. Free fluoride ion is found in pentafluorophenyllithium solutions at temperatures above  $-20^\circ\text{C}$  and the formation of tetrafluorobenzene is indicated by subsequent reaction chemistry [11]. Therefore, even when  $\text{LiC}_6\text{F}_5$  is prepared immediately before use and maintained at temperatures below  $-20^\circ\text{C}$ , as in the present study, it is possible that the C–F bond activation processes that result in the for-

mation of the  $[\text{ZrF}_2(\text{C}_6\text{F}_5)_5]^{2-}$  ion do not involve the transition metal.

#### 4. Experimental

All operations were carried out under vacuum or under argon using standard Schlenk techniques. Pentafluorobenzene (PCR), 12-crown-4 (Fluka), and zirconium tetrachloride (Cerac) were used as received.  $N,N,N',N'$ -tetramethylethylenediamine (Aldrich) was distilled from sodium. Diethylether was distilled from sodium/benzophenone immediately before use. NMR studies were performed using a Varian Unity 400 spectrometer.  $^1\text{H}$ - and  $^{19}\text{F}$ -NMR chemical shifts are reported in  $\delta$  units (positive chemical shifts to high frequency) relative to  $\text{SiMe}_4$  or  $\text{CFCl}_3$ . IR spectra were recorded on a Perkin–Elmer 599B instrument as Nujol mulls between KBr plates. Microanalyses were carried out by the Microanalytical Laboratory of the School of Chemical Sciences at the University of Illinois.

##### 4.1. Bis(1,4,7,10-tetraoxacyclododecane)lithium tetrakis(pentafluorophenyl)dichlorozirconate(IV); $[\text{Li}(12\text{-crown-4})_2]_2[\text{ZrCl}_2(\text{C}_6\text{F}_5)_4]$ (**1**)

To a solution of pentafluorobenzene (2.2 ml, 19.8 mmol) in diethylether (50 ml) at  $-78^\circ\text{C}$  was added butyllithium (11 ml of a 1.6 M solution in hexanes, 17.6 mmol) dropwise over 30 min. The solution was stirred at  $-78^\circ\text{C}$  for 3 h. The resulting colorless mixture was added to a slurry of  $\text{ZrCl}_4$  (0.62 g, 2.66 mmol) in diethylether (20 ml) at  $-20^\circ\text{C}$ . The resulting suspension was stirred at  $-20^\circ\text{C}$  for 3 h. The solvent was removed under vacuum at  $-20^\circ\text{C}$  and the resulting white precipitate was extracted with diethylether (100 ml). The extract was filtered and treated with 12-crown-4 (1.7 ml, 10.64 mmol). The cloudy white mixture was cooled to  $-20^\circ\text{C}$  to afford colorless crystals of the product which were isolated by filtration. Yield: 0.80 g (23%). Anal. Calc. for  $\text{C}_{56}\text{H}_{64}\text{Cl}_2\text{F}_{20}\text{Li}_2\text{O}_{16}\text{Zr}$ : C, 43.4; H, 4.13; Cl, 4.58; Li, 0.96; Zr, 5.88. Found: C, 42.3; H, 3.79; Cl, 4.77; Li, 0.83; Zr, 6.39%.  $^1\text{H}$ -NMR spectra obtained by adding toluene- $d_8$  to samples of **1** only showed peaks due to  $\text{C}_6\text{F}_5\text{H}$  [ $^1\text{H}$ -NMR: 5.79 (m);  $^{19}\text{F}\{^1\text{H}\}$ -NMR:  $\delta$  164.8 (t ‘t’,  $^3J_{\text{FF}} = 20$ ,  $^4J_{\text{FF}} = 7.5$  Hz, *m*-CF),  $-156.9$  (t,  $^3J_{\text{FF}} = 20$  Hz, *p*-CF),  $-140.8$  (d ‘t’,  $^3J_{\text{FF}} = 19$ ,  $^4J_{\text{FF}} = 9.4$  Hz, *o*-CF)] and peaks due to free 12-crown-4. [ $^1\text{H}$ -NMR:  $\delta$  3.45 (s)]. IR ( $\text{cm}^{-1}$ ): 2924 s, 2855 s, 2361 w, 1655 w, 1629 w, 1533 m, 1468 s, 1435 s, 1417 m, 1377 m, 1366 m, 1307 w, 1290 w, 1246 m, 1136 s, 1100 s, 1062 m, 1044 s, 1026 m, 1001 m, 970 m, 947 m, 929 m, 853 w, 803 w, 710 m, 669 w, 540 w, 477 w.

4.2. *Bis(N,N,N',N'-tetramethylethylenediamine)lithium (N,N,N',N'-tetramethylethylenediamine)lithium pentakis(pentafluorophenyl)difluorozirconate(IV); [Li(tmed)<sub>2</sub>][Li(tmed)]<sub>2</sub>[ZrF<sub>2</sub>(C<sub>6</sub>F<sub>5</sub>)<sub>3</sub>] (2)*

To a solution of pentafluorobenzene (3.2 ml, 28.4 mmol) in diethylether (50 ml) at  $-78^{\circ}\text{C}$  was added butyllithium (16 ml of a 1.6 M solution in hexanes, 25.3 mmol) dropwise over 30 min. The solution was stirred at  $-78^{\circ}\text{C}$  for 3 h. The resulting very pale yellow mixture was transferred by cannula to a slurry of ZrCl<sub>4</sub> (0.89 g, 3.82 mmol) in diethylether (20 ml) at  $-20^{\circ}\text{C}$ . The resulting suspension was stirred at  $-20^{\circ}\text{C}$  for 3 h, and then the solvent was removed under vacuum. The resulting white precipitate was extracted with diethylether (100 ml), the extract was filtered, and the filtrate was treated with *N,N,N',N'*-tetramethylethylenediamine (2.3 ml, 15.28 mmol). The resulting deep blue solution was cooled to  $-20^{\circ}\text{C}$  to afford colorless crystals of the product which were isolated by filtration. Yield: 0.75 g (18%). Anal. Calc. for C<sub>54</sub>H<sub>64</sub>F<sub>27</sub>Li<sub>3</sub>N<sub>8</sub>Zr: C, 44.7; H, 4.41; Li, 1.53; N, 7.72; Zr, 6.28. Found: C, 42.3; H, 3.00; Li, 1.71; N, 6.07; Zr, 6.49; Cl, <0.3%. Attempts to obtain the NMR spectrum of this compound gave results similar to those described above. IR (cm<sup>-1</sup>): 2924 s, 2722 m, 2307 w, 2261 w, 2162 w, 2021 w, 1959 w, 1809 w, 1628 s, 1603 s, 1429 br s, 1290 s, 1231 s, 1185 s, 1161 s, 1129 s, 1100 s, 1035 br s, 943 s, 835 w, 789 s, 775 s, 733 m, 712 m, 594 s, 529 s, 475 s.

4.3. *Crystallographic studies [52]*

Single crystals of [Li(12-crown-4)<sub>2</sub>]<sub>2</sub>[ZrCl<sub>2</sub>(C<sub>6</sub>F<sub>5</sub>)<sub>4</sub>] (1), grown from diethylether, were mounted on glass fibers with Paratone-N oil (Exxon) and immediately cooled to  $-75^{\circ}\text{C}$  in a cold nitrogen gas stream on a Siemens SMART CCD diffractometer (Single crystals of [Li(tmed)<sub>2</sub>][Li(tmed)]<sub>2</sub>[ZrF<sub>2</sub>(C<sub>6</sub>F<sub>5</sub>)<sub>3</sub>]<sub>1/2</sub>Et<sub>2</sub>O (2), grown from diethylether, were treated similarly. Subsequent comments in parentheses will refer to this compound). Standard peak search and indexing procedures gave rough cell dimensions, and least-squares refinement yielded the cell dimensions given in Table 1.

Data were collected with an area detector by using the measurement parameters listed in Table 1. Systematic absences for  $0k0$  ( $k \neq 2n$ ) and  $h0l$  ( $h + l \neq 2n$ ) were only consistent with space group  $P2_1/n$ . The measured intensities were reduced to structure factor amplitudes and their estimated S.D. values by correction for background and Lorentz and polarization effects. Corrections for crystal decay were unnecessary, but an absorption correction was applied. Systematically absent reflections were deleted and symmetry equivalent reflections were averaged to yield the set of unique data. A total of 7805 unique data were measured; the 0

4 18,  $-12\ 6\ 2$ ,  $-9\ 2\ 3$ , and  $-4\ 14\ 10$  reflections had  $F_o^2 < -3\sigma(F_o^2)$  and were suppressed, leaving 7801 that were used in the least-squares refinement (For 2, the reflections at high angles were weak, so only those reflections with  $\theta < 22.5^{\circ}$  were included in the least-squares refinement. A total of 8967 data with  $\theta < 22.5^{\circ}$  were measured. Subsequently, the 0 1 1, 0 2 0, and 0 3 1 reflections were found to have been occluded by the beam stop and 202 other reflections had  $F_o^2 < -3\sigma(F_o^2)$ ; these reflections were suppressed. The remaining 8762 data were used in the least-squares refinement).

The structure was solved using direct methods (SHELXS-86). The correct positions for all the atoms in the anion and many of the atoms in the two cations were deduced from an E-map (For 2, the structure was solved by direct methods (SHELXTL). The correct positions for the zirconium, ring carbon, and fluorine atoms were deduced from an E-map). Subsequent least-squares refinement and difference Fourier calculations revealed the positions of the remaining non-hydrogen atoms. One of the 12-crown-4 molecules was disordered in two conformations, and a site occupancy factor for the major conformer refined to 0.54(1) (For 2, three of the four tmed ligands in the asymmetric unit were disordered; in addition, a diethylether molecule was disordered about the origin. Site occupancy factors for C61A, C62A, C91A–C96A, O1, and C101–C104 were set to 0.5; a site occupancy factor for N3A, N4A, and C71A–C76A was refined and converged to 0.606(5). The sum of the occupancy for the A and B sites was set to 1). The quantity minimized by the least-squares program was  $\Sigma w(F_o^2 - F_c^2)^2$ , where  $w = \{[\sigma(F_o^2)]^2 + (0.0954P)^2 + 0.0153P\}^{-1}$  and  $P = (F_o^2 + {}^2F_c^2)/3$  (For 2,  $\Sigma w(F_o^2 - F_c^2)^2$ , where  $w = \{[\sigma(F_o^2)]^2 + (0.072P)^2\}^{-1}$ ). The analytical approximations to the scattering factors were used, and all structure factors were corrected for both real and imaginary components of anomalous dispersion. The carbon atoms of the C<sub>6</sub>F<sub>5</sub> rings were refined as ideal hexagons with C–C = 1.39 Å, and the fluorine atoms were fixed in 'idealized' positions with C–F = 1.35 Å. In the one disordered 12-crown-4 molecule, the C–O and C–C distances within each disordered component were restrained to values of 1.45(3) and 1.54(3) Å, respectively, while the 1,3 C···O and C···C distances were restrained to values of 2.47(5) and 2.40(5) Å, respectively (For 2, the C<sub>6</sub>F<sub>5</sub> rings were constrained to similar geometries within 0.03 Å, the *meta*- and *para*-fluorine atoms were fixed in 'idealized' positions with C–F = 1.35 Å, and the C–C distances involving the *para*-carbon atoms were constrained to be exactly equal; a parameter to represent this latter distance was refined. For the tmed ligands, the N–C distances involving disordered carbon atoms were restrained to 1.47(3) Å, the C–C distances involving



disordered carbon atoms were restrained to 1.54(3) Å, and for cases in which both carbon atoms were disordered the 1,3 C⋯C distances within each disordered component were restrained to 2.40(5) Å. All hydrogen atoms were fixed in 'idealized' positions with C–H = 0.99 Å for methylene hydrogens and C–H = 0.98 Å for methyl hydrogen atoms. The lithium atoms were refined isotropically, a common isotropic displacement parameter was refined for the non-hydrogen atoms of the disordered 12-crown-4 molecule, and all other non-hydrogen atoms were refined with independent anisotropic displacement parameters (For **2**, a common isotropic displacement parameter was refined for all partial-occupancy carbon atoms; the lithium atoms and the disordered nitrogen atoms were given independent isotropic displacement parameters, and all other non-hydrogen atoms were refined anisotropically). The displacement parameters for the methylene hydrogen atoms were set equal to 1.2 times  $U_{\text{iso}}$  or  $U_{\text{eq}}$  for the attached carbon atom, while those for the methyl hydrogen atoms were set equal to 1.5 times  $U_{\text{iso}}$  or  $U_{\text{eq}}$  for the attached carbon atom. Successful convergence was indicated by the maximum shift/error of 0.004 [0.002] for the last cycle. Final refinement parameters are given in Table 1. The largest peak in the final Fourier difference map ( $0.60 \text{ e } \text{Å}^{-3}$ ) was located 0.61 Å from F22 (For **2**, the largest peak in the final Fourier difference map ( $0.57 \text{ e } \text{Å}^{-3}$ ) was located midway between atoms C91A,B and C92A,B).

A final analysis of variance between observed and calculated structure factors showed no apparent errors.

## 5. Supplementary material

Crystallographic data have been deposited with the Cambridge Crystallographic Data Centre, CSD Nos. CCDC 118862 and 118863 for compounds **1** and **2**. Copies of this information may be obtained free of charge from The Director, CCDC, 12 Union Road, Cambridge CB2 1EZ, UK (fax: +44-1223-336-033; e-mail: deposit@ccdc.cam.ac.uk).

## Acknowledgements

We thank the Department of Energy under Grant DEFG02-91ER45439 for support of this work and Dr Scott R. Wilson and Teresa Prussak-Wieckowska of the University of Illinois Materials Chemistry Laboratory for collecting the X-ray data sets.

## References

- [1] A.L. Galyer, G. Wilkinson, J. Chem. Soc. Chem. Commun. (1972) 318.
- [2] A.J. Shortland, G. Wilkinson, J. Chem. Soc. Dalton Trans. (1973) 872.
- [3] A.L. Galyer, G. Wilkinson, J. Chem. Soc. Dalton Trans. (1976) 2235.
- [4] J.C. Green, D.R. Lloyd, L. Galyer, K. Mertis, G. Wilkinson, J. Chem. Soc. Dalton Trans. (1978) 1403.
- [5] P.M. Morse, G.S. Girolami, J. Am. Chem. Soc. 114 (1989) 4114.
- [6] M.M. Olmstead, P.P. Power, S.C. Shoner, Organometallics 7 (1988) 1380.
- [7] R.J. Morris, G.S. Girolami, Organometallics 10 (1991) 792.
- [8] R. Hoffmann, J.W. Howell, A.R. Rossi, J. Am. Chem. Soc. 98 (1976) 2484.
- [9] A. Haaland, A. Hammel, K. Rypdal, H.V. Volden, J. Am. Chem. Soc. 112 (1990) 4547.
- [10] V. Pfennig, K. Seppelt, Science 271 (1996) 626.
- [11] P.L. Coe, R. Stephens, J.C. Tatlow, J. Chem. Soc. (1962) 3227.
- [12] G.S. Brenner, D.F. Hinkley, L.M. Perkins, S. Weber, J. Chem. Soc. (1964) 2385.
- [13] K. Prout, T.S. Cameron, R.A. Forder, S.R. Critchley, B. Denton, G.V. Rees, Acta Crystallogr. Sect. B 30 (1974) 2290.
- [14] P.P. Power, Acc. Chem. Res. 21 (1988) 147.
- [15] P. Jutzi, M. Meyer, H.V. Rasika Dias, P.P. Power, J. Am. Chem. Soc. 112 (1990) 4841.
- [16] A. Blaschette, D.H. Nagel, P.G. Jones, Z. Naturforsch. B 49 (1994) 36.
- [17] R.B. VonDreele, J.J. Stezowski, R.C. Fay, J. Am. Chem. Soc. 93 (1971) 2887.
- [18] H.J. Hurst, J.C. Taylor, Acta Crystallogr. Sect. B 26 (1970) 417.
- [19] I.P. Kondratyuk, R.L. Bukvetskii, R.L. Davidovich, M.A. Medkov, Koord. Khim. 8 (1982) 218.
- [20] M.A. Bush, G.A. Sim, J. Chem. Soc. A (1971) 2225.
- [21] E.F. Murphy, T. Lubben, A. Herzog, H.W. Roesky, A. Demisar, M. Noltemeyer, H.G. Schmidt, Inorg. Chem. 35 (1996) 23.
- [22] G. Brunton, Acta Crystallogr. Sect. B 27 (1971) 1944.
- [23] A. Antinolo, M.F. Lappert, A. Singh, D.J.W. Winterborn, L.M. Engelhardt, C.L. Raston, A.H. White, A.J. Carty, N.J. Taylor, J. Chem. Soc. Dalton Trans. (1987) 1463.
- [24] R. Bortolin, V. Patel, I. Munday, N.J. Taylor, A.J. Carty, J. Chem. Soc. Chem. Commun. (1985) 456.
- [25] W.H. Howard, G. Parkin, Polyhedron 12 (1993) 1253.
- [26] B.D. Santarsiero, E.J. Moore, Acta Crystallogr. Sect. C 44 (1988) 433 This pseudo nine-coordinate zirconium hydroxide has a much longer Zr–O distance of 2.554(3) Å.
- [27] S. Hao, S. Gambarotta, C. Bensimon, J. Am. Chem. Soc. 114 (1992) 3556.
- [28] K. Jonas, K.R. Porshke, C. Kruger, Y.H. Tsay, Angew. Chem. Int. Ed. Engl. 15 (1976) 621.
- [29] R.J. Morris, G.S. Girolami, Organometallics 8 (1989) 1478.
- [30] J.L. Kiplinger, T.G. Richmond, C.E. Osterberg, Chem. Rev. 94 (1994) 373.
- [31] F.A. Cotton, R.M. Wing, J. Organomet. Chem. 9 (1967) 511.
- [32] S.C. Cohen, A.G. Massey, Adv. Fluor. Chem. 8 (1970) 235.
- [33] M.R. Churchill, T.A. O'Brien, J. Chem. Soc. A (1968) 2970.
- [34] H.H. Murray, J.P. Fackler, L.C. Porter, D.A. Briggs, M.A. Guerra, R.J. Lagow, Inorg. Chem. 26 (1987) 357.
- [35] A. Clearfield, R. Gopal, I. Bernal, G.A. Moser, M.D. Rausch, Inorg. Chem. 14 (1975) 2727.
- [36] P.M. Treichel, M.A. Chaudhari, F.G.A. Stone, J. Organomet. Chem. 1 (1963) 98.
- [37] G.A. Razuvaev, V.N. Latyaeva, G.A. Kilyakova, G.Ya. Mal'kova, Dokl. Akad. Nauk. SSSR 191 (1970) 620.
- [38] J.D. Scollard, D.H. McConville, S.J. Rettig, Organometallics 16 (1997) 1810.
- [39] M.J. Nelsen, G.S. Girolami, in preparation.
- [40] R. Hoffman, B.F. Beier, E.L. Muettterties, A.R. Rossi, Inorg. Chem. 16 (1977) 511.

- [41] Z. Lin, I. Bytheway, *Inorg. Chem.* 35 (1996) 594.
- [42] D.L. Kepert, *Inorganic Stereochemistry*, Springer-Verlag, New York, 1982.
- [43] N.M. Doherty, N.W. Hoffman, *Chem. Rev.* 91 (1991) 553.
- [44] M. Witt, M. Roesky, H.W. Roesky, *Prog. Inorg. Chem.* 40 (1992) 353.
- [45] P.L. Watson, T.H. Tulip, I. Williams, *Organometallics* 9 (1990) 1999.
- [46] C.J. Burns, R.A. Andersen, *J. Chem. Soc. Chem. Commun.* (1989) 136.
- [47] M. Aizenberg, D. Milstein, *Science* 265 (1994) 359.
- [48] M. Aizenberg, D. Milstein, *J. Am. Chem. Soc.* 117 (1995) 8674.
- [49] J.H. Holloway, E.G. Hope, *J. Fluor. Chem.* 76 (1996) 209.
- [50] M. Hudlicky, *J. Fluor. Chem.* 44 (1989) 345.
- [51] L.E. Schock, C.P. Brock, T.J. Marks, *Organometallics* 6 (1987) 232.
- [52] For a description of the crystallographic procedures and programs used, see: J.A. Jensen, S.R. Wilson, G.S. Girolami, *J. Am. Chem. Soc.* 110 (1988) 4977.